JP Journal of Heat and Mass Transfer
© 2025 Pushpa Publishing House, Prayagraj, India
https://pphmjopenaccess.com
https://doi.org/10.17654/0973576325050 **P-ISSN: 0973-5763**
Volume 38, Number 6, December 2025, Pages 953-975 **E-ISSN: 3049-2556**

MODELING OF AN UNSTEADY TWO-PHASE FLOW OVER A LINEAR INCLINED STRETCHING SHEET WITH CONSIDERATION OF TRANSVERSE FORCE AND ELECTRIFICATION OF PARTICLES

Debasis Mishra and Tumbanath Samantara*

School of Applied Science
Centurion University of Technology and Management
752050, Odisha, India

Abstract

In this article, the problem of a two-phase unsteady boundary layer flow past an inclined stretched surface has been considered. The impact of electrification and transverse force has been analyzed in presence of Buoyancy force. The fluid is neither electrified externally nor is considered in electric medium rather the electrification occurred due to the collision of particles between particle-particle, particle-fluid and particle-wall. A balanced mathematical model has been formulated with account of the two-phase boundary layer flow of fluid which consists of systems of highly nonlinear partial differential equations. An appropriate similarity transformation has been used for

Received: October 24, 2025; Revised: November 24, 2025; Accepted: December 10, 2025
Keywords and phrases: two-phase flow, electrification, inclined stretching sheet, bvp4c.
*Corresponding author

How to cite this article: Debasis Mishra and Tumbanath Samantara, Modeling of an unsteady two-phase flow over a linear inclined stretching sheet with consideration of transverse force and electrification of particles, JP Journal of Heat and Mass Transfer 38(6) (2025), 953-975.
https://doi.org/10.17654/0973576325050

Published Online: December 16, 2025

converting the system of equations into ordinary differential equations and solved numerically by the use of bvp4c tool of MATLAB. Moreover, the influence of electrification parameter, angle of inclination, transverse force, fluid particle interaction parameter and others on flow and heat transformation characteristics has been analyzed graphically and analytically. The results are in agreement with the existing results.

1. Introduction

The problems of electrification as well as the transverse force and unsteady boundary layer flow of fluid over an inclined stretching sheet have vast practical application on the field of engineering and sciences. Stretching sheet has a vast practical application on the field of engineering and sciences. In many manufacturing processes like polymer and plastic processing, wire and fiber drawing, hot rolling and metal casting, the role of inclined stretching sheet has significant impact on the quality of final product. Also, the rate of stretching has been playing a tremendous role in manufacturing process like extrusion of fiber, plastic and metal sheet, paper and glass fiber production also. Due to a very large expanse practical application of fluid flow over stretched sheet, in last three to four decades, many researchers have extended their research interest towards the fluid flow over a stretchable surface with the effect of electrification, angle of inclination and transverse force.

The first ever explosion about the boundary layer flow behavior over a continuous hard surface was studied by Sakiadis [1, 2]. On account of various mechanical applications in industry, Crane [3] has investigated the uniform flow over the sheet. The idea of Crane is considered by various experts for their various applications over the stretching surface. The heat transfer characteristics of continuous stretching surface have been analyzed by Grubka and Bobba [4]. Chen [5] expanded on this work by investigating the impact of heat generation and thermal radiation in power-law fluids, highlighting the role of energy exchange in such systems. Further, the study of unsteady stretching surfaces has been critical in understanding dynamic systems where the flow and heat transfer change over time. Samantara [6] investigated on the velocity profile of the fluid particle suspension over a horizontal plate. Makinde and Aziz [7] examined heat and mass transfer in an MHD (magnetohydrodynamic) mixed convection flow over a vertical plate in a porous medium, addressing the effects of thermal radiation and chemical reactions. Furthermore, studies by Ishak et al. [8] focused on the heat transfer characteristics over an unsteady stretching permeable surface, which has practical relevance in engineering applications. Kanungo and Samantara [9, 10] have examined the effect of electrification, radiation and other physical parameter with the unsteady flow of fluid over a stretching sheet. Dusty fluids, which are mixtures of gases and suspended particles, have been another focal point of research. The exploration of nanofluids and their thermal properties has gained prominence in recent years due to their enhanced heat transfer capabilities. Pati et al. [11] investigated the effects of chemical reaction, Brownian motion, thermophoresis and nanoparticle electrification on Cu-water nanofluid flow past a plate. Mishra et al. [12] have been focused on the study of effect of electrification and transverse force on two-phase steady flow which passed over a vertical stretching sheet. Mishra et al. [13] investigated the effects of Brownian motion, thermophoresis and nanoparticle electrification with slip conditions on Cu-water nanofluid flow past a plate. Choi and Eastman [14] introduced the concept of enhancing the thermal conductivity of fluids by adding nanoparticles, which has since been a major area of research. Buongiorno et al. [15] conducted a benchmark study on the thermal conductivity of nanofluids, providing foundational data on their performance. Tripathy et al. [16-18] have analyzed the mathematical and numerical modeling of two-phase mixed convective heat transfer over an exponential stretching sheet and non-uniform grid with effect of radiation. Khan and Pop [19] further contributed by studying the boundary-layer flow of a nanofluid past a stretching sheet, emphasizing the effect of nanoparticles on heat transfer and flow dynamics. Pati et al. [24, 25] have also investigated the heat and mass transfer on natural convective boundary layer with effect of electrified nanoparticles.

Hence, in this article, a numerical and graphical investigation has been carried out for a two-phase unsteady boundary layer flow of fluid over an inclined stretching sheet with effect of electrification and transverse force. Again the consideration of transverse force and electrification in momentum equation of the particle phase, when the fluid is passed over an inclined stretching sheet, are not available in literature. So we consider these combinations for current investigation.

2. Formulation of the Problem

Assume that the two-dimensional unsteady flow of fluid flows near a boundary layer across the inclined stretching sheet as shown in Figure 1. The dusty fluid which is available on the surface began moving by the sudden movement of stretching sheet with an angle α. The wall is stretched linearly with velocity $u = U_w(x, t) = \frac{cx}{1 - at}$, due to the application of two interacting opposite forces on the wall. The co-ordinates (x, y) are assumed as, x axis is considered along the flow direction and the y axis makes an angle α to the wall. With the above conditions and Boussinesq boundary layer approximations, the leading governing equations of continuity and momentum for both fluid and particle phases [9, 10] are as follows:

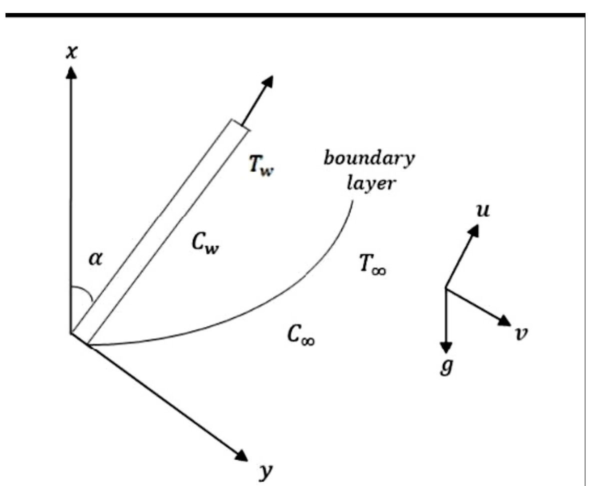

Figure 1. Physical model of present research problem.

$$\frac{\partial u}{\partial x} + \frac{\partial v}{\partial y} = 0, \tag{1}$$

$$\frac{\partial}{\partial t}\rho_p + \frac{\partial}{\partial x}(\rho_p u_p) + \frac{\partial}{\partial y}(\rho_p v_p) = 0, \tag{2}$$

$$\begin{aligned}(1-\varphi)\rho\left(\frac{\partial u}{\partial t} + u\frac{\partial u}{\partial x} + v\frac{\partial u}{\partial y}\right) = {} & (1-\varphi)\mu\frac{\partial^2 u}{\partial y^2} - \frac{1}{\tau_p}\varphi\rho_s(u-u_p) \\ & + (1-\varphi)\rho g\beta^*(T-T_\infty)\cos\alpha \\ & + \varphi\rho_s\left(\frac{e}{m}\right)E,\end{aligned} \tag{3}$$

$$\begin{aligned}\varphi\rho_s\left(\frac{\partial u_p}{\partial t} + u_p\frac{\partial u_p}{\partial x} + v_p\frac{\partial u_p}{\partial y}\right) = {} & \frac{\partial}{\partial y}\left(\varphi\mu_s\frac{\partial u_p}{\partial y}\right) + \frac{1}{\tau_p}\varphi\rho_s(u-u_p) \\ & + \varphi\frac{0.73(\rho/\rho_s)^{1/2}}{\tau_p^{1/2}}\left|\frac{\partial u}{\partial y}\right|^{1/2}(u-u_p) \\ & + \varphi\rho_s\left(\frac{e}{m}\right)E,\end{aligned} \tag{4}$$

$$\varphi\rho_s\left(\frac{\partial v_p}{\partial t} + u_p\frac{\partial v_p}{\partial x} + v_p\frac{\partial v_p}{\partial y}\right) = \frac{\partial}{\partial y}\left(\varphi\mu_s\frac{\partial v_p}{\partial y}\right) + \frac{1}{\tau_p}\varphi\rho_s(v-v_p), \tag{5}$$

with boundary conditions

$$\left.\begin{aligned} & u = U_w(x,t) = \frac{cx}{1-at},\ v = V_w(x,t) = -\frac{v_0}{\sqrt{1-at}} \text{ at } y = 0 \\ & \rho_p = \omega\rho,\ u = 0,\ u_p = 0,\ v_p \to v \text{ as } y \to \infty \end{aligned}\right\}, \tag{6}$$

where

$U = u_w(x,t) = \frac{cx}{1-at}$ is the velocity in x direction, $V_w(x) = -\frac{v_0}{\sqrt{1-at}}$ is the wall velocity in y direction, (u, v) and (u_p, v_p) are velocity components of fluid and particle phase along the x and y axes, respectively, (ρ, ρ_p) is the density for fluid and particle phases, ω is the density ratio in the mainstream, (μ, μ_s) are coefficients of viscosity, (τ_p) is the velocity and thermal equilibrium time of the particle cloud, (φ) is finite volume fraction, (ρ_s) is the material density of particle, and (β^*) is the coefficient of thermal expansion. Other symbols have their usual meaning. A set of following similarity transformation has been used for both the phase of continuity and momentum equation to convert into the system of ordinary differential equations in the form of *f*, *F*, *G*, *H* and the similarity variable η:

$$\left.\begin{aligned} u &= \frac{cx}{1-at} f'(\eta),\ v = -\sqrt{\frac{c\nu}{1-at}} f(\eta),\ \frac{\varphi\rho_s}{\rho} = \frac{\rho_p}{\rho} = \rho_r = H(\eta) \\ u_p &= \frac{cx}{1-at} F(\eta),\ v_p = \sqrt{\frac{c\nu}{1-at}} G(\eta),\ \eta = \sqrt{\frac{c}{\nu(1-at)}} y \end{aligned}\right\}. \tag{7}$$

Substituting (7) in equations (2)-(5), we have

$$f''' = A\left(f' + \frac{\eta}{2} f''\right) + f'^2 - ff'' + \frac{1}{(1-\varphi)} \beta H(f' - F)$$

$$- \lambda\theta\cos\alpha - \frac{1}{(1-\varphi)} HE, \tag{8}$$

$$F'' = \frac{1}{\varepsilon}\left[a\left(\frac{\eta}{2} F' + F\right) + F^2 + GF' - 0.73\sqrt{\beta} F_t \sqrt{f''}(f' - F) - M\right], \tag{9}$$

$$G'' = \frac{1}{\varepsilon}\left[\frac{A}{2}(\eta G' + G) + GG' + \beta(f + G)\right], \tag{10}$$

$$H' = -\frac{(HF + HG')}{\left(\frac{\eta}{2} A + G\right)}, \tag{11}$$

with boundary condition

$$G' = 0,\ f = 0,\ f' = 1 \text{ as } \eta \to 0,$$

$$F' = 0,\ F = 0,\ G = -f,\ H = \omega \text{ as } \eta \to \infty, \tag{12}$$

where $\gamma = \frac{\rho_s}{\rho}$ is the material density of the particles, $\beta = \frac{1}{c\tau_p}$ is the interaction parameter of the fluid particles, and $\varepsilon = \frac{\nu_s}{\nu}$ is the diffusion parameter.

3. Temperature Equation Analysis

The continuous stretching of the wall generates heat at the surface and the temperature is given by $T = T_w = T_\infty + T_0 \frac{cx^2}{1 - at}$, where T_∞ is the temperature of an ambient fluid. Thus the governing temperature equations with conduction and electrification for both of the phases are given by

$$(1-\varphi)\rho c_p\left(\frac{\partial T}{\partial t} + u\frac{\partial T}{\partial x} + v\frac{\partial T}{\partial y}\right)$$

$$= (1-\varphi)k\frac{\partial^2 T}{\partial y^2} + \frac{1}{\tau_T}\varphi\rho_s c_s(T_p - T) + \frac{1}{\tau_p}\varphi\rho_s(u - u_p)^2$$

$$+ (1-\varphi)\mu\left(\frac{\partial u}{\partial y}\right)^2 + \varphi\rho_s\left(\frac{e}{m}\right)Eu_p, \tag{13}$$

$$\varphi\rho_s c_s\left(\frac{\partial T_p}{\partial t} u_p\frac{\partial T_p}{\partial x} + v_p\frac{\partial T_p}{\partial y}\right)$$

$$= \frac{\partial}{\partial y}\left(\varphi k_s\frac{\partial T_p}{\partial y}\right) - \frac{1}{\tau_T}\varphi\rho_s c_s(T_p - T) - \frac{1}{\tau_p}\varphi\rho_s(u - u_p)^2$$

$$+ \varphi\mu_s\left[u_p\frac{\partial^2 u_p}{\partial y^2} + \left(\frac{\partial u_p}{\partial y}\right)^2\right] + \varphi\rho_s\left(\frac{e}{m}\right)Eu_p, \tag{14}$$

with boundary condition

$$T = T_w = T_\infty + T_0\frac{cx^2}{\nu(1-at)^2} \text{ at } y = 0,$$

$$T \to T_\infty,\ T_P \to T_\infty \text{ as } y \to \infty. \tag{15}$$

For most of the gases

$$\tau_p = \tau_T, \quad k_s = k\frac{c_s}{c_p}\frac{\mu}{\mu_p}, \quad \frac{c_s}{c_p} = \frac{2}{3Pr}.$$

Introduce the following non-dimensional similarity transformations:

$$\theta(\eta) = \frac{T - T_\infty}{T_w - T_\infty}, \quad \theta_p(\eta) = \frac{T_p - T_\infty}{T_w - T_\infty}, \tag{16}$$

where

$$T = T_\infty + T_0\frac{cx^2}{\nu(1-at)^2}\theta(\eta), \; T_p = T_\infty + T_0\frac{cx^2}{\nu(1-at)^2}\theta_p(\eta). \tag{17}$$

The heat transfer equations (13) and (14) are converted to

$$\theta'' = \begin{bmatrix} Pr(2f'\theta - f\theta') + \frac{2}{3}\frac{1}{(1-\varphi)}\beta H(\theta_p - \theta) \\ -\frac{1}{(1-\varphi)}\beta PrEcH(F - f')^2 - PrEcf''^2 \\ +\frac{A}{2}Pr(\eta\theta' + 4\theta) - \frac{1}{(1-\varphi)}PrEcHMF \end{bmatrix}, \tag{18}$$

$$\theta_p'' = \frac{1}{\frac{\varepsilon}{pr}}\begin{bmatrix} \frac{A}{2}(\eta\theta_p - 4\theta_p) + 2F\theta_p + G + \beta(\theta_p - \theta) \\ +\frac{3}{2}\beta PrEc(f - F)^2 \\ -\frac{3}{2}\varepsilon PrEc(FF'' - F'^2) - \frac{3}{2}PrEcHMF \end{bmatrix}, \tag{19}$$

with boundary condition

$$\theta = 1, \; \theta_p' = 0 \text{ as } \eta \to 0, \; \theta \to 0, \; \theta_p \to 0 \text{ as } \eta \to \infty. \tag{20}$$

4. Numerical Computation

The system of equations (7)-(10) with the boundary conditions (12) and equations (13)-(14) with boundary conditions (15) are computed by applying the numerical method “Shooting Technique” followed by Runge-Kutta 4th order method which is unconditionally stable. It is computed by using bvp4c tool of MATLAB by considering the finite value of $\eta \to \infty$ say $\eta = 15$ with a particular tolerance level of less than $O(10^{-6})$. The numerical and graphical representation has been made for the impact of different physical parameters like unsteady parameter (A), electrification parameter (M), Prandtl number (Pr), angle of inclination parameter (α), buoyancy parameter (λ) and the transverse force (Tr).

Table 1. Result validating table

Prandtl number (Pr)	[20]	[21]	[22]	[5]	[4]	[23]	Current study
0.72	———	1.0885	1.0885	1.0885	1.0885	1.0885	1.0884
1.0	1.3333	1.3333	1.3333	1.3333	1.3333	1.3333	1.3333
3.0	2.5097	-------	2.5097	2.5097	-------	2.5097	2.5097
10.0	4.7969	4.7969	4.7969	4.7969	4.7969	-------	4.7969

The results are also matched with the results available in previous literature as Ishak et al. [20], Abel et al. [21], Gireesha et al. [22], Chen [5], Grubka and Bobba [4] and Mukhopadhyay and Andersson [23] as shown in Table 1. Here the values of rate of heat transfer are matched with the previous authors. So, it proves the validation of our programme.

5. Results and Discussion

Figures 2 and 3 represent the effects of angle of inclinations on velocity profile of fluid phase and particle phase. From the figures, it is observed that the angle of inclinations has very negligible effects on velocity profile of fluid as well as particle phase. Raising the value of angle of inclinations decreases the velocity of fluid phase as well as particle phase. Moreover, it is observed that the velocity falls rapidly in particle phase as compared to fluid phase which is of natural phenomena. Figures 4 and 5 represent the effects of angle of inclinations on temperature profile of fluid phase and particle phase. The effects on fluid phase are almost negligible and have very little effects at the boundary layer away from surface. But in the case of particle phase, the effects of angle of inclinations are prominent towards away from the surface. The temperature of particle phase falls as the angle of inclinations increases. This happens due to slow down of the particles by raising the inclined stretching sheet.

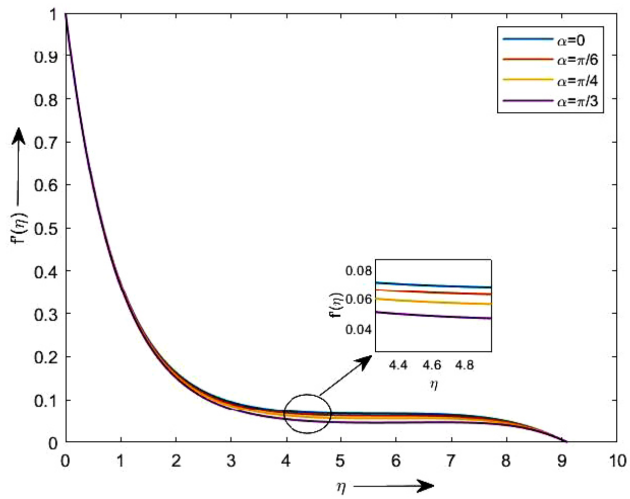

Figure 2. Effect of angle of inclination (α) on fluid velocity.

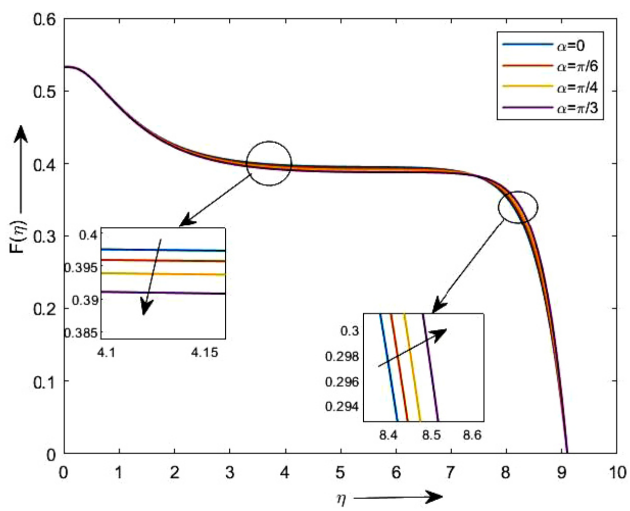

Figure 3. Effect of angle of inclination (α) on particle velocity.

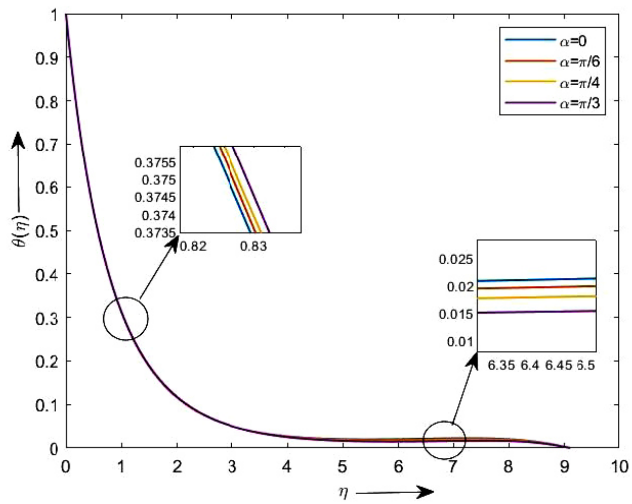

Figure 4. Effect of angle of inclination (α) on fluid temperature.

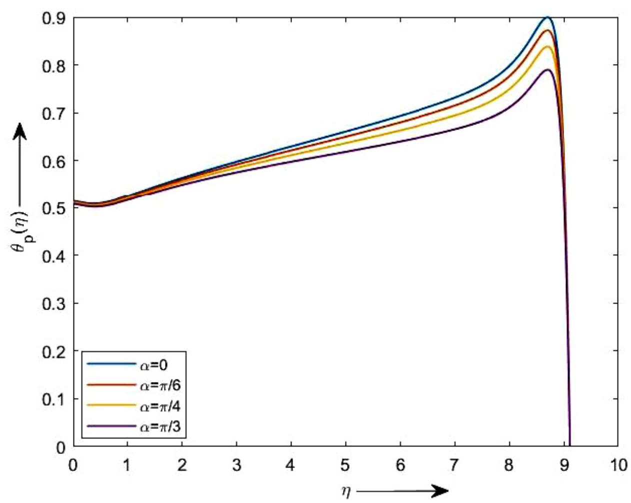

Figure 5. Effect of angle of inclination (α) on particle temperature.

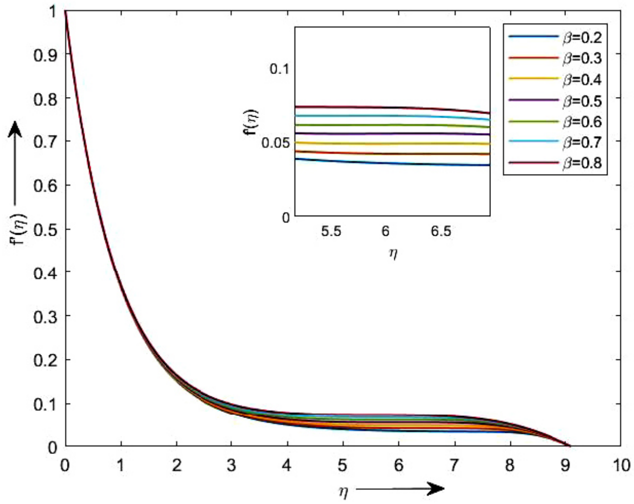

Figure 6. Effect of fluid-particle interaction parameter (β) on fluid velocity.

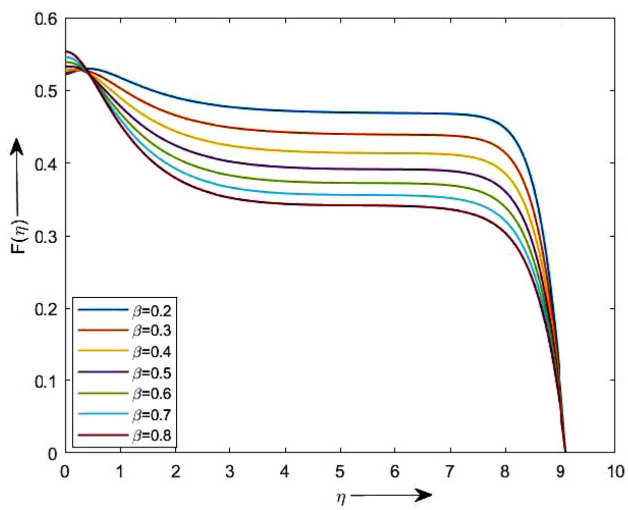

Figure 7. Effect of fluid-particle interaction parameter (β) on particle velocity.

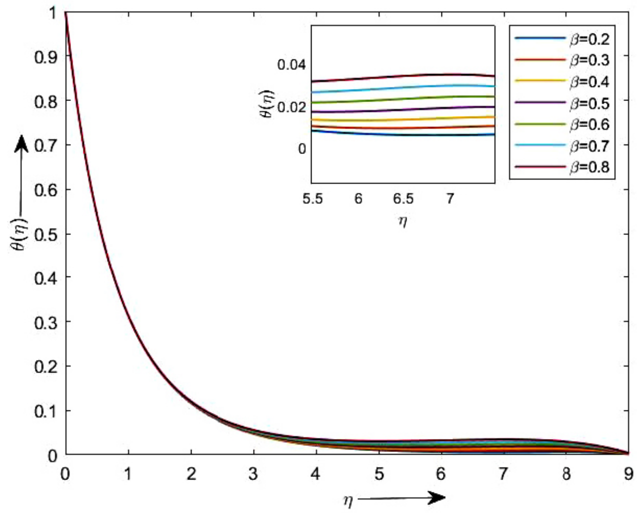

Figure 8. Effect of fluid-particle interaction parameter (β) on fluid temperature.

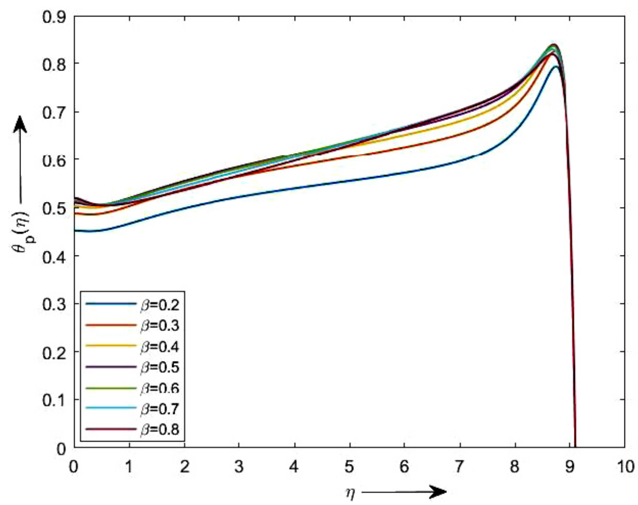

Figure 9. Effect of fluid-particle interaction parameter (β) on particle temperature.

From Figures 6 and 7, it is concluded that the velocity of fluid phase is inversely proportional with the particle-particle interaction parameter (β) in the region of boundary layer. The particle interaction parameter has negligible effect on the free stream, however, it accelerates the motion of fluid at near the sheet. But in the case of particle phase, the situation is just opposite and has very negligible effects. The effects start visible little away from sheet as compared to the case of fluid phase. Figures 8 and 9 represent the variation of temperature profile of fluid phase and particle phase. It is observed that the temperature of fluid rises with rise of the value of the interaction parameter (β) at the middle region of the boundary layer but it is very less significant. Again, the sudden fall of curve indicates the fall of fluid temperature, due to absorption of heat by particles from the fluid. But in case of particle phase, the temperature of particles rises with increasing the value of interaction parameter (β) as fluid phase but it is more prominent in case of particle phase.

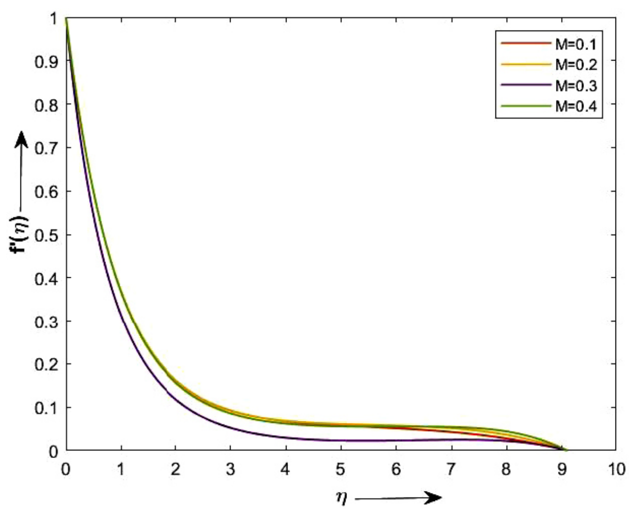

Figure 10. Effect of electrification parameter (M) on fluid velocity.

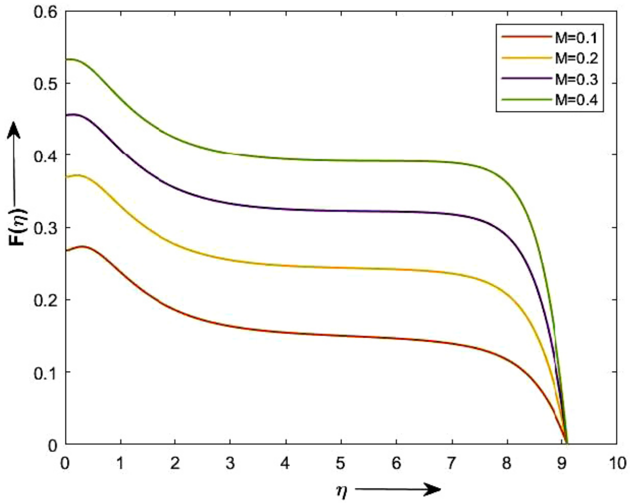

Figure 11. Effect of electrification parameter (M) on particle velocity.

Figures 10 and 11 represent the effect of electrification on velocity profile of fluid phase and particle phase. From the figures, it is concluded that the velocity of fluid phase increases with increasing of electrification. However, the effect is quite opposite in case of particle phase. As the electrification parameter increases, the particle velocity decreases, although the distinguishing is very small.

Figures 12 and 13 represent the effect of electrification on temperature profile of fluid phase and particle phase. From the figure, it is observed that the temperature profile of fluid phase falls suddenly due to absorption of heat by the particles from the fluid. The electric current produced here is due to collision of particles and not supplied from outside. It is also observed that the temperature of fluid increases with increase of electrification parameter (M) in the boundary layer. But in case of particle phase, the effect is prominent. The temperature profile of particle phase rises with increasing of the electricity parameter.

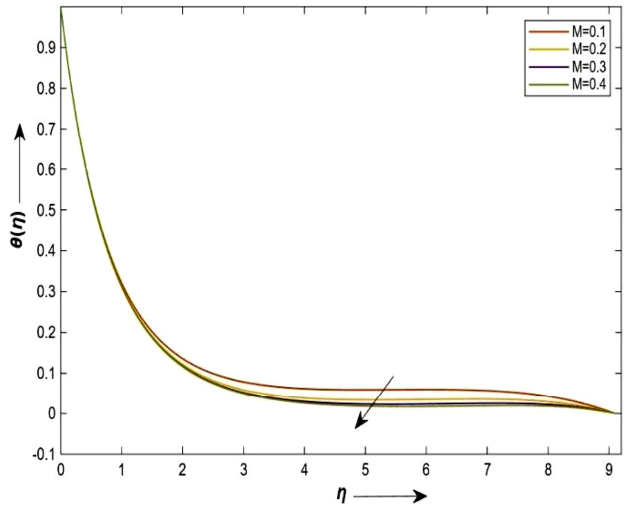

Figure 12. Effect of electrification parameter (M) on fluid temperature.

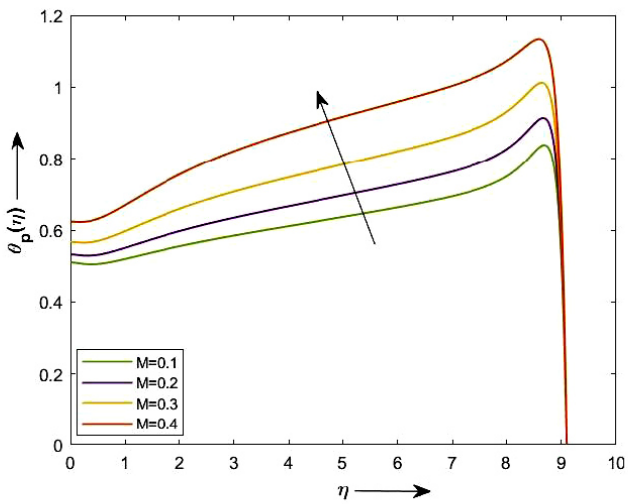

Figure 13. Effect of electrification parameter (M) on particle temperature.

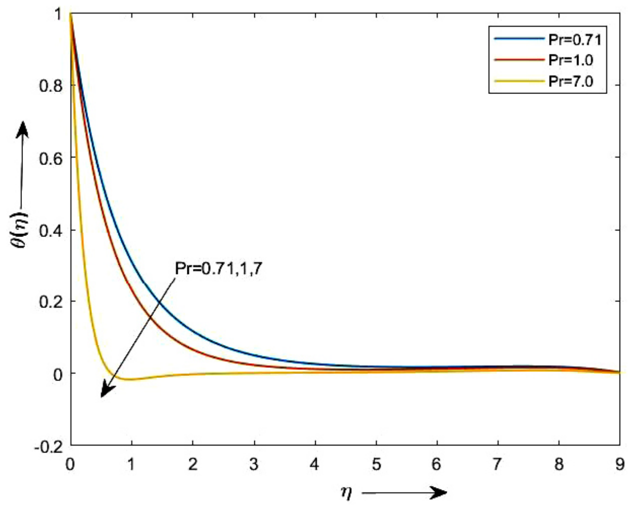

Figure 14. Effect of Prandtl number (Pr) on fluid temperature.

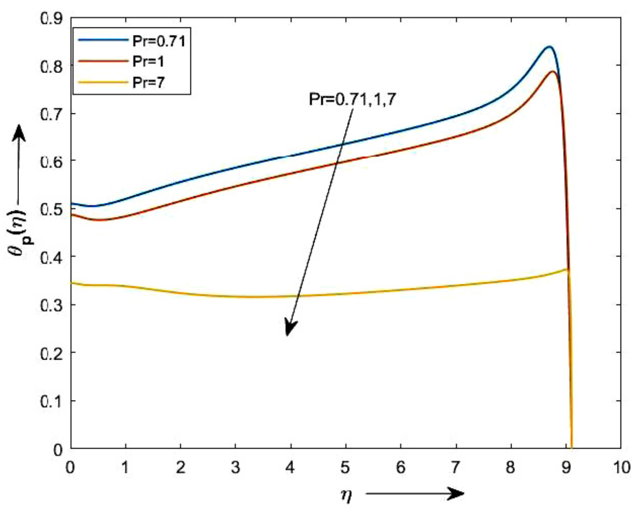

Figure 15. Effect of Prandtl number (Pr) on particle temperature.

Figures 14 and 15 represent the effect of Prandtl number on temperature profile of fluid phase and particle phase. From the figure, it is concluded that as the Prandtl number increases, the temperature of fluid phase as well as particle phase decreases. The increasing value of Prandtl number happens whenever the thermal diffusivity decreases which causes decreasing in fluid as well as particle temperature.

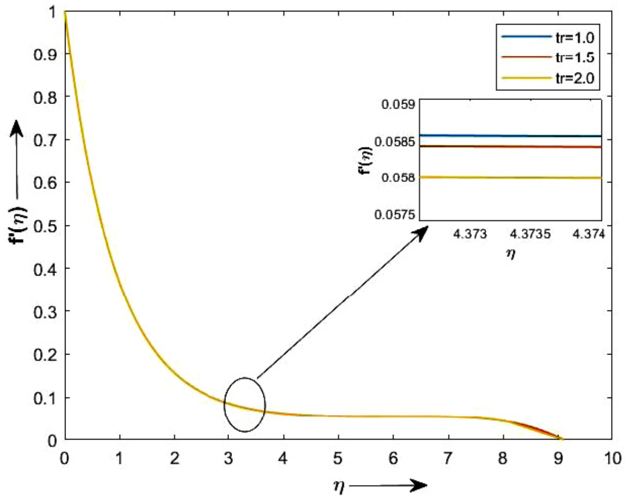

Figure 16. Effect of transverse force (Tr) on fluid velocity.

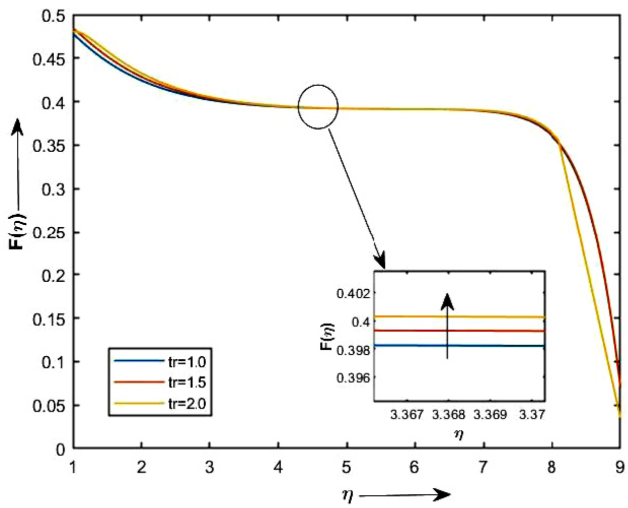

Figure 17. Effect of transverse force (Tr) on fluid velocity.

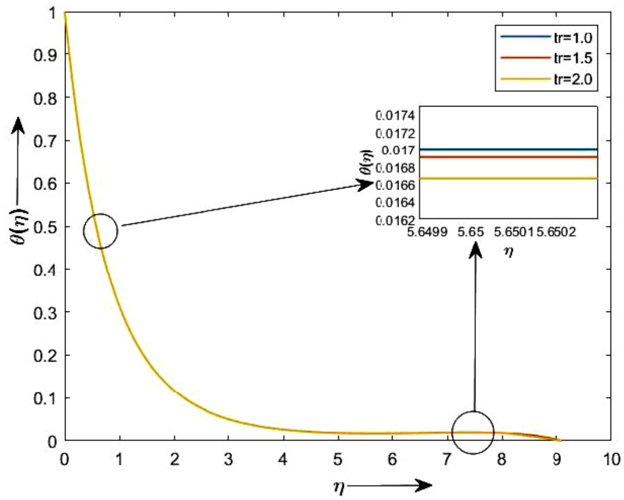

Figure 18. Effect of transverse force (Tr) on fluid temperature.

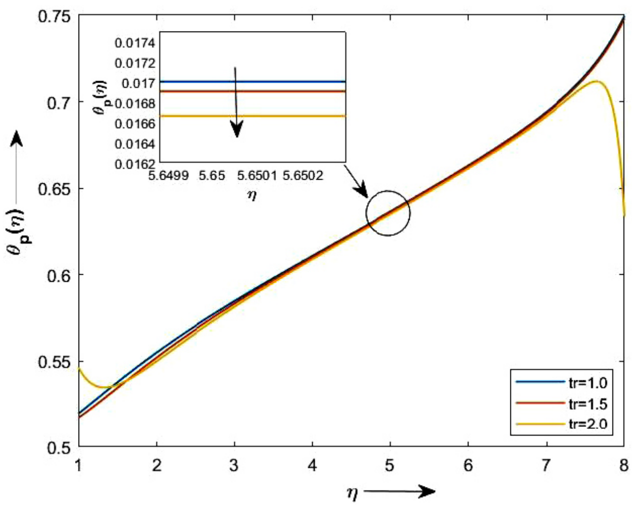

Figure 19. Effect of transverse force (Tr) on particle temperature.

A transverse force is a force that acts perpendicular to direction of flow. Figures 16 and 17 represent the effect of transverse force on velocity profile of fluid phase and particle phase. From the figure, it is found that it has very negligible effects in the velocity profile of fluid phase and particle phase. However, in particle phase, the velocity profile has little distinctions for different value of (Tr) during lower and upper parts of boundary layer. In general, velocity of fluid was influenced by transverse force. This increases with increase in (Tr). Opposite effects happen towards free stream. Figures 18 and 19 represent the effect of transverse force on temperature profile of fluid phase and particle phase, respectively. From the figure, it is observed that it has very negligible effects in the temperature profile of fluid phase and particle phase. It is found in both the phases that the temperature of fluid and particle falls with rise of transverse force parameter. It is little remarkable in particle phase.

Table 2. Skin friction $(f''(0))$ and Nusselt number $(-\theta'(0))$ with different parameters

Pr	α	M	Tr	β	$f''(0)$ Skin friction	$-\theta'(0)$ Nusselt number
0.71	$\frac{\pi}{4}$	0.4	1.0	0.5	1.36855	1.61403
1.0					1.36855	1.84261
7.0					1.36855	5.12535
0.71	0	0.4	1.0	0.5	1.36724	1.61398
	$\frac{\pi}{6}$				1.36784	1.61400
	$\frac{\pi}{4}$				1.36855	1.61403
	$\frac{\pi}{3}$				1.36947	1.61406
0.71	$\frac{\pi}{4}$	0.1	1.0	0.5	1.38968	1.61359
		0.2			1.38028	1.61456
		0.3			1.37360	1.61451
		0.4			1.36855	1.61403
0.71	$\frac{\pi}{4}$	0.4	1	0.5	1.36855	1.61403
			1.5		1.36926	1.61392
			2.0		1.40338	1.61380
0.71	$\frac{\pi}{4}$	0.4	0.5	0.2	1.36636	1.61296
				0.3	1.36707	1.61331
				0.4	1.36780	1.61366
				0.5	1.36855	1.61403

6. Conclusion

The above table considered the effects of various parameters like Prandtl number (Pr), angle of inclination (α), electrification parameter (M), transverse force (tr) and fluid particle interaction parameter (β) on skin friction $(f''(0))$ and Nusselt number $(\theta'(0))$. It is observed that the rate of heat transfer increases with increase in Prandtl number (Pr) whereas no change occurs in skin friction rate. On the other hand, angle of inclination shows an impact on both the skin friction and heat transfer rate. With the increase in angle, both the skin friction and heat transfer rate increase gradually. With increase in electrification parameter (M), the skin friction and heat transfer rate behave in contrast to each other as the skin friction decreases and rate of heat transfer increases gradually. As transverse force (tr) increases, the skin friction increases but the rate of heat transfer decreases slightly. The impact of fluid particle interaction parameter (β) shows a significant behavior on both the skin friction and heat transfer. Both increase with increase in (β).

Acknowledgement

We thank the anonymous referees for their comments and feedback on earlier version of this document.

References

[1] B. C. Sakiadis, Boundary-layer behavior on continuous solid surfaces: I. boundary-layer equations for two-dimensional and axisymmetric flow, AIChE Journal 7(1) (1961), 26-28.

[2] B. C. Sakiadis, Boundary-layer behavior on continuous solid surfaces: the boundary layer on a continuous flat surface, AIChE Journal 7(2) (1961), 221-225.

[3] L. J. Crane, Flow past a stretching plate, Z. Angew. Math. Phys. ZAMP 21(4) (1970), 645-647.

[4] L. Grubka and K. Bobba, Heat transfer characteristics of a continuous stretching surface with variable temperature, Journal of Heat Transfer 107(1) (1985), 248-250.

[5] C.-H. Chen, Laminar mixed convection adjacent to vertical, continuously stretching sheets, Heat and Mass Transfer 33(5) (1998), 471-476.

[6] T. Samantara, Velocity profile of fluid particle suspension over a horizontal plate with electrification of particles, International Journal of Innovative Technology and Exploring Engineering 8(11) (2019), 1119-1122.

[7] O. D. Makinde and A. Aziz, Boundary layer flow of a nanofluid past a stretching sheet with a convective boundary condition, International Journal of Thermal Sciences 50(7) (2011), 1326-1332.

[8] A. Ishak, R. Nazar and I. Pop, Heat transfer over an unsteady stretching permeable surface with prescribed wall temperature, Nonlinear Anal. Real World Appl. 10(5) (2009), 2909-2913.

[9] S. Kanungo and T. Samantara, Numerical solution of two-phase radiated unsteady flow over a horizontal stretching sheet with simultaneous effect of electrification, radiation and non-uniform internal heat source/sink, Journal of Advanced Research in Fluid Mechanics and Thermal Sciences 100(3) (2022), 11-22.

[10] S. Kanungo and T. Samantara, Flow and heat transfer of unsteady two-phase boundary layer flow past an inclined permeable stretching sheet with electrification of particles, CFD Lett. 15(5) (2023), 134-144.

[11] A. K. Pati, M. M. Rout, R. Sahu, I. S. Ramakoti, K. K. Panda and K. C. Sethi, Chemical reaction, electrification, Brownian motion and thermophoresis effects of copper nanoparticles on nanofluid flow with skin friction, heat and mass transfer, East European Journal of Physics 2024(4) (2024), 152-158.

[12] J. Mishra, T. Samantara and P. Tripathy, Effects of electrification and transverse force on dusty flow over a linear stretching sheet, CFD Lett. 16 (2023), 151-161.

[13] S. Mishra, A. K. Pati, A. Misra and S. K. Mishra, Thermal performance of nanofluid flow along an isothermal vertical plate with velocity, thermal, and concentration slip boundary conditions employing Buongiorno's revised non-homogeneous model, East European Journal of Physics 2024(4) (2024), 98-106.

[14] S. U. Choi and J. A. Eastman, Enhancing thermal conductivity of fluids with nanoparticles, Technical report, Argonne National Lab.(ANL), Argonne, IL (United States), 1995.

[15] J. Buongiorno et al., A benchmark study on the thermal conductivity of nanofluids, Journal of Applied Physics 106(9) (2009), 094312.

[16] P. K. Tripathy, T. Samantara, J. Mishra and S. Panda, Mixed convective radiative heat transfer in a particle-laden boundary layer fluid over an exponentially stretching permeable surface, AIP Conf. Proc. 2435 (2022), 020-030.

[17] S. K. Mishra and P. K. Tripathy, Mathematical and numerical modeling of two phase flow and heat transfer using non-uniform grid, Far East J. Appl. Math. 54(2) (2011), 107-126.

[18] P. K. Tripathy, T. Samantara and S. Kanungo, Radiation effect on convective boundary layer dusty flow over a stretching surface, AIP Advances 14(3) (2024), 035151.

[19] W. Khan and I. Pop, Boundary-layer flow of a nanofluid past a stretching sheet, International Journal of Heat and Mass Transfer 53(11-12) (2010), 2477-2483.

[20] A. Ishak, R. Nazar and I. Pop, Hydromagnetic flow and heat transfer adjacent to a stretching vertical sheet, Heat and Mass Transfer 44(8) (2008), 921-927.

[21] M. S. Abel, P. Siddheshwar and M. M. Nandeppanavar, Heat transfer in a viscoelastic boundary layer flow over a stretching sheet with viscous dissipation and nonuniform heat source, International Journal of Heat and Mass Transfer 50(5-6) (2007), 960-966.

[22] B. J. Gireesha, G. S. Roopa and C. S. Bagewadi, Boundary layer flow of an unsteady dusty fluid and heat transfer over a stretching sheet with non-uniform heat source/sink, Engineering 3 (2011), 726-735.

[23] S. Mukhopadhyay and H. I. Andersson, Effects of slip and heat transfer analysis of flow over an unsteady stretching surface, Heat and Mass Transfer 45(11) (2009), 1447-1452.

[24] A. K. Pati, A. Misra and S. K. Mishra, Thermal analysis of Ag-water nanofluid flow induced by a horizontally stretching cylinder with electrified nanoparticles, Sigma: Journal of Engineering and Natural Sciences/Mühendislik ve Fen Bilimleri Dergisi 43(4) (2025), 1152-1165.

[25] A. K. Pati, A. Misra and S. K. Mishra, Heat and mass transfer analysis on natural convective boundary layer flow of a Cu-water nanofluid past a vertical flat plate with electrification of nanoparticles, Advances and Applications in Fluid Mechanics 23(1) (2019), 1-15.